Photochemistry of (η^3-Allyl)tricarbonylcobalt in Frozen Gas Matrices at 12 K. Infrared Spectroscopic Evidence for the Formation of (η^3-Allyl)-dicarbonylcobalt, (η^3-Allyl)dicarbonyl(dinitrogen)cobalt, (σ-Allyl)-tetracarbonylcobalt, and Tetracarbonylcobalt Complexes †

Antony J. Rest * and David J. Taylor
Department of Chemistry, The University, Southampton SO9 5NH

Infrared spectroscopic evidence is presented to show that photolysis of [Co(η^3-allyl)(CO)$_3$] in gas matrices at 12 K gives [Co(η^3-allyl)(CO)$_2$] (in Ar or CH_4), [Co(η^3-allyl)(CO)$_2$(N_2)] (in N_2), and [Co(σ-allyl)(CO)$_4$] followed by [Co(CO)$_4$] (in CO). The detection of [Co(η^3-allyl)(CO)$_2$] is consistent with the results of kinetic studies, which have been interpreted in terms of a dissociative path and a co-ordinatively unsaturated intermediate in the thermal CO substitution reactions, and theoretical calculations which show a low M–C(O) bond order. The detection of [Co(σ-allyl)(CO)$_4$] and the reversibility of the reaction [Co(η^3-allyl)(CO)$_3$] + CO $\rightleftharpoons$ [Co(σ-allyl)(CO)$_4$] suggest that there may be a contribution to the reactivity of [Co(η^3-allyl)(CO)$_3$] from the hitherto neglected associative path.

Kinetic studies of the CO exchange and substitution reactions of transition metal carbonyl complexes have established two types of reaction path: (*a*) a dissociative path, *cf.* S_N1, involving primary CO loss and the formation of a co-ordinatively unsaturated species, and (*b*) an associative path, *cf.* S_N2, where the rate-determining step is the addition of the incoming ligand L to form an expanded co-ordination number species.[1,2] The majority of complexes follow the dissociative path, a minority follow the associative path, and some show a combination of both paths.[1,2] The path followed can be related to the substituents bound to the metal in isoelectronic complexes. For example, in [Ni(CO)$_4$][3] and [Co(η^3-allyl)-(CO)$_3$][4] rapid replacement of CO by phosphines occurs, by the dissociative path, while [Co(CO)$_3$(NO)][5] and [Fe(η^3-allyl)-(CO)$_2$(NO)][6] undergo slow reactions by the associative path with an additional small contribution from the dissociative path for [Co(CO)$_3$(NO)].[5]

Qualitative correlations,[1,2] which exist between reactivity and metal–ligand [M–C(O)] bond strength in a number of cases for the dissociative mechanism, have been placed on firmer foundations by recent theoretical studies,[7–10] which have sought to correlate both reactivity and S_N1/S_N2 character with theoretical parameters. In the series of complexes [Cr(η^6-C_6H_6)(CO)$_3$], [Mn(η^5-C_5H_5)(CO)$_3$], [Fe(η^4-C_4H_4)-(CO)$_3$], and [Co(η^3-allyl)(CO)$_3$], decreases in the M–C(O) overlap populations and π^* orbital populations (SCCC–MO calculations)[9] and Wiberg indices (CNDO/2 calculations)[10] in the series Cr > Mn > Fe > Co led to the prediction of an increasing importance for the S_N1 path from Cr to Co. The greatest tendency for S_N2 behaviour was found[9] for Cr and Mn *via* attack of the incoming ligands at the metals. There was, however, some inhibition[9] to this process, because of the requirement to form a seven-co-ordinate transition state species, on account of the small sizes of these first-row transition elements. Calculations (SCCC–MO) showed[7] that the M–C(O) total overlap population of [Co(η^5-C_5H_5)(CO)$_2$] was significantly higher than that of [Co(η^3-allyl)(CO)$_3$]. These differences were attributed to the electron-donating ability of the η^5-C_5H_5 ligand *versus* the electron-accepting tendency of the η^3-allyl ligand, together with differing geometries in the complexes. The electron-acceptor ability of the η^3-allyl ligand led to weakening of the M–C(O) bonds, which is consistent with fast S_N1 reactions for [Co(η^3-allyl)(CO)$_3$][4] as compared with slow S_N2 reactions for [Co(η^5-C_5H_5)(CO)$_2$].[11] Other calculations (semi-empirical MO)[8] have indicated that the [Co(CO)$_3$] fragment in [Co(η^3-allyl)(CO)$_3$] has asymmetric bonding, with one CO group more weakly bonded to the metal, and that this leads to the relatively high reactivity of [Co(η^3-allyl)(CO)$_3$][4] as compared with [Fe(η^3-allyl)(CO)$_2$(NO)][6] and [Co(CO)$_3$-(NO)].[5]

Proton n.m.r. studies of η^3-allylmetal complexes have shown that the η^3-allyl ligands are stereochemically non-rigid. At some low temperature the η^3-allyl ligand appears to be 'static' (AA'BB'X pattern), while at some higher temperature the spectrum collapses to a 'dynamic' spectrum (AX_4 pattern) owing to a rapid intramolecular rearrangement that causes the AA' (*anti*) and BB' (*syn*) protons to become equivalent. A careful examination[12] of the possible mechanisms, which could lead to the observed proton equilibration, has led to the accepted conclusion that the η^3-allyl group becomes σ-bonded to the metal in the crucial transition state, *i.e.* a σ-allyl group. In this transition state, rotation about the M–C bond followed by re-formation of the η^3 form best accounts for the stereochemical non-rigidity. Equilibria of the type η^3-allyl $\rightleftharpoons$ σ-allyl are presumably also crucial to the importance of metal–allyl complexes in organic synthesis[13] and catalysis.[13–15] Such an equilibrium and comparable ones for other multidentate polyenes, *e.g.* η^5-C_5H_5 $\rightleftharpoons$ η^3-C_5H_5, do not appear to have been considered in discussions of the mechanisms of CO exchange and substitution reactions. Such polyene hapticity changes could avoid the inhibiting[9] need for seven-co-ordination number species in S_N2 reactions of small first-row transition metal elements.

Low-temperature matrix isolation studies have led to the generation and characterisation of a variety of species which have been proposed as intermediates in organometallic reaction mechanisms.[16] Most of the species have been formed by CO ejection from metal carbonyls and substituted metal carbonyls. Recently, however, unstable species have been reported which show changes in the mode of co-ordination of cyclic and open-chain polyenes, *e.g.* the formation of [Co(η^3-C_5H_5)(CO)$_3$] from [Co(η^5-C_5H_5)(CO)$_2$],[17] and of [Fe(η^2-1,3-C_4H_6)(CO)$_3$] from [Fe(η^4-1,3-C_4H_6)(CO)$_3$].[18] The former species is consistent with the associative (S_N2) path proposed[11] for the CO ligand substitution reactions of [Co(η^5-C_5H_5)(CO)$_2$].

In this paper we report a matrix isolation study of the

† *Non-S.I. units employed:* 1 Torr = (101 325/760) Pa; 1 atm = 101 325 Pa.

Table 1. Terminal metal–carbonyl stretching band positions (cm^{-1}) for $[Co(\eta^3\text{-allyl})(CO)_3]$ and its photoproducts in Ar, CH_4, N_2, and CO matrices at 12 K

Complex	Matrix			
	Ar	CH_4	N_2	CO
$[Co(\eta^3\text{-allyl})(CO)_3]$	2 072.6	2 066.8	2 070.7	2 068.0
	2 005.2 [a]	1 998.6 [a]	2 002.8 [a]	2 000.2 [a]
$[Co(\eta^3\text{-allyl})(CO)_2]$	2 037.5	2 032.9		
	1 966.9	1 959.8		
$[Co(\eta^3\text{-allyl})(CO)_2(N_2)]$ [b]			2 031.9	
			1 980.5	
$[Co(\sigma\text{-allyl})(CO)_4]$				2 103.0
				2 037.6
				2 020.9
				2 012.3
$[Co(CO)_4]$				2 028.0
				2 009.9

[a] Weighted mean band position. [b] ν_{NN} at 2 241.0 cm^{-1}

primary photochemical reactions of $[Co(\eta^3\text{-allyl})(CO)_3]$ in unreactive (CH_4 or Ar) and reactive (N_2 or CO) matrices at 12 K. We relate the results to those of kinetic and theoretical studies of CO exchange and substitution reactions.

Experimental

Details of the 12 K cryostat, infrared and u.v.–visible spectrometers, photolysis source, and matrix gases have been given elsewhere.[17]

$[Co(\eta^3\text{-allyl})(CO)_3]$ was prepared by the reaction of allyl bromide with $Na[Co(CO)_4]$ in dry tetrahydrofurane at low temperature.[19] Final purification was achieved by vacuum-line transfer and drying over phosphorus pentaoxide. Matrices were prepared by making gas mixtures of $[Co(\eta^3\text{-allyl})(CO)_3]$ and matrix gas of the required composition for monomer isolation (1 : 2000 to 1 : 5000), using a vacuum line and standard manometric techniques, and depositing the gas mixture on to the cooled CsI window by the pulsed technique. The pulsing volume was 10 cm^3 and the pulsing pressure was in the range 80—150 Torr, *i.e.* 0.05—0.09 mmol of gas per pulse. Typically 20—30 pulses of gas mixture were deposited to give optically transparent matrices.

Wavelength-selective photolysis was achieved with combinations of absorbing materials: filter A, $\lambda < 280$ and $\lambda > 550$ nm, quartz gas cell (pathlength 25 mm) containing Cl_2 (2 atm) + quartz gas cell (pathlength 25 mm) containing Br_2 (200 Torr); filter B, $\lambda > 320$ nm, soda glass disc (thickness 5 mm).

Results

Photolysis of $[Co(\eta^3\text{-allyl})(CO)_3]$ *in* Ar *and* CH_4 *matrices at* 12 K.—On deposition, the i.r. spectra of $[Co(\eta^3\text{-allyl})(CO)_3]$ isolated at high dilution (1 : 2000) in Ar [Figure 1(a)] and CH_4 matrices at 12 K consisted of two strong bands in the terminal CO stretching region at positions (Table 1) which correspond closely with the two bands (2065.0m and 1998.0s cm^{-1}) observed in solution.[19] Two strong bands in the terminal CO stretching region were also observed for N_2 [Figure 2(a)] and CO [Figures 3(a) and 4(a)] matrices. The gas-phase electron diffraction data for $[Co(\eta^3\text{-allyl})(CO)_3]$ could not be fitted satisfactorily if it was assumed that the $[Co(CO)_3]$ fragment had three-fold local symmetry.[20] Better agreement was obtained for a molecule with C_s symmetry. The structure showed that one OC–Co–CO angle was larger (109°) than the other two

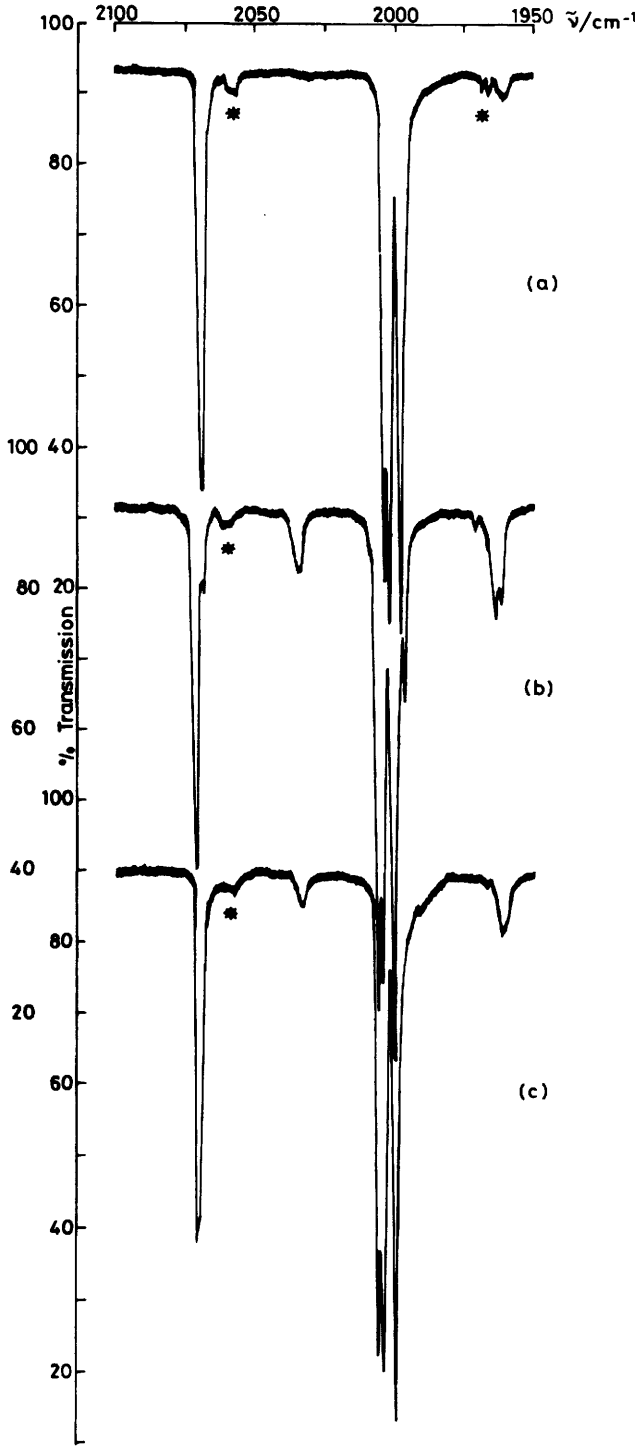

Figure 1. Infrared spectra from an experiment with $[Co(\eta^3\text{-allyl})(CO)_3]$ isolated at high dilution in an Ar matrix at 12 K: (a) after deposition, (b) after 90 min u.v. irradiation (filter A), and (c) after further 40 min long-wavelength irradiation (filter B); bands marked with an asterisk are due to $[Co(\eta^3\text{-allyl})(^{12}CO)_2(^{13}CO)]$ present in natural abundance

(100°) but that all the Co–C(O) bonds were of equal length.[20] In a theoretical study [8] it was also noted that the $[Co(CO)_3]$ fragment was asymmetric, with one CO group more weakly bonded to the metal. It was assumed [8] that the more weakly bonded CO ligand was the one lost in the S_N1 substitution

reactions. A C_s symmetry $[Co(CO)_3]$ fragment should give rise to *three* i.r.-active CO stretching bands (A', A', and A'') whereas a fragment with C_{3v} local symmetry should give rise to *two* bands (A_1 and E). Some [M(polyene)$(CO)_3$] complexes show three well separated bands in solution and in gas matrices at 12 K, *e.g.* $[Mo(\eta^6\text{-}C_7H_8)(CO)_3]$.[21,22] The series of complexes $[Cr(\eta^6\text{-}C_6H_6)(CO)_3]$, $[Mn(\eta^5\text{-}C_5H_5)(CO)_3]$, and $[Fe(\eta^4\text{-}C_4H_4)(CO)_3]$, however, show two bands in solution with the lower wavenumber band broader than the upper band. In gas matrices at 12 K this series of complexes showed fine structure in the lower wavenumber band [23] similar to that seen in the lower wavenumber of $[Co(\eta^3\text{-allyl})(CO)_3]$ in gas matrices [Figures 1(a)—4(a)]. The observation of two bands has led to the $[M(CO)_3]$ fragments being assigned C_{3v} local symmetry, and this assignment has been satisfactorily used in sophisticated theoretical calculations.[9,10] In matrix isolation studies the packing of host matrix molecules around large substrate molecules leads to splittings in bands, which vary from band to band for a given matrix and from matrix to matrix for any given molecule.[24] The splitting patterns for the lower band of $[Co(\eta^3\text{-allyl})(CO)_3]$ are within the normal range (0—10 cm^{-1}) for matrix splitting effects.[24] Until such effects are better understood, it seems reasonable to treat the lower band of $[Co(\eta^3\text{-allyl})(CO)_3]$ as a single fundamental and to designate the $[Co(CO)_3]$ fragment as having C_{3v} local symmetry. Band positions in Table 1 are, therefore, given as weighted mean positions. These weighted mean band positions (Table 1) were used to calculate [25] energy-factored terminal CO stretching (K) and interaction (k_i) force constants in Ar, CH_4, N_2, and CO matrices (Table 2). Relative intensities of the two bands in Ar, CH_4, N_2, and CO matrices ($R = I_{A_1}/I_E$) were obtained by tracing, cutting out, and weighing bands recorded in absorbance mode. These relative intensities were used to calculate bond angles (θ) for the $[Co(CO)_3]$ fragment using the expression $I_{sym}/I_{antisym} (= R) = [3\cot^2(\theta/2) - 1]/4$.[25] The values (100°; Table 2) are consistent with the average bond angle value (103°) found for $[Co(\eta^3\text{-allyl})(CO)_3]$ by electron diffraction studies and for $[Co\{\eta^3\text{-}C_3(C_6H_5)_3\}(CO)_3]$ [104° (average)] obtained recently by *X*-ray diffraction studies.[26] The good correlation supports the assignment of C_{3v} local symmetry for the $[Co(CO)_3]$ fragment in i.r. studies. The weak bands (marked with an asterisk) in all cases (Figures 1—4) are due to $[Co(\eta^3\text{-allyl})(^{12}CO)_2(^{13}CO)]$ present in natural abundance.

A period of u.v. photolysis with the filtered medium-pressure Hg arc (filter A), corresponding to the u.v. electronic absorption bands of $[Co(\eta^3\text{-allyl})(CO)_3]$ (222, 254, 265, and 276 nm; Figure 5), produced similar spectra in both Ar and CH_4 matrices [Figure 1(b)]. New terminal CO stretching bands were observed at 2037.5 and 1966.9 cm^{-1} (Ar) and 2032.9 and 1959.8 cm^{-1} (CH_4). Additionally there was a weak band (2138.0 cm^{-1}) in each matrix which is not illustrated in the Figures. This band may be assigned to photochemically generated 'free' CO. Photolysis with long-wavelength radiation (filter B) slowly caused regeneration of the parent bands at the expense of the product absorptions [Figure 1(c)].

The relative intensities of the new terminal carbonyl bands remained constant under a variety of photolysis cycles, *i.e.* growing and decreasing at the same rate, indicating that they arose from a single product species. The dilution used (*ca.* 1 : 2000 to 1 : 5000) and the reversibility of the matrix reaction rule out the possibility of any aggregate formation. The most probable explanation for the new product bands is that they are the A_1 and B_1 terminal CO stretching modes of $[Co(\eta^3\text{-allyl})(CO)_2]$ which has C_{2v} local symmetry for the $[Co(CO)_2]$ fragment. This result is analogous to the formation of $[Cr(\eta^6\text{-}C_6H_6)(CO)_2]$, $[Mn(\eta^5\text{-}C_5H_5)(CO)_2]$, and $[Fe(\eta^4\text{-}C_4H_4)(CO)_2]$ in Ar and CH_4 matrices at 12 K.[23] The band positions

Table 2. Energy-factored CO stretching (K) and interaction (k_i) force constants (N m^{-1}),[a] experimental intensity ratios (R),[a] and estimated bond angles (θ)[a] for $[Co(\eta^3\text{-allyl})(CO)_3]$ and its photoproducts in Ar, CH_4, and N_2 matrices at 12 K together with comparison data for $[Fe(\eta^4\text{-}C_4H_4)(CO)_3]$ and its photoproducts

Complex	Parameter	Matrix Ar	CH_4	N_2
$[Co(\eta^3\text{-allyl})(CO)_3]$	K	1 661.5	1 651.1	1 657.7
	k_i	37.0	37.3	37.2
	R	0.2818	0.2600	0.2753
	θ	99.8	101.0	100.1
$[Co(\eta^3\text{-allyl})(CO)_2]$	K	1 620.1	1 610.7	
	k_i	57.1	59.0	
	R	0.5529	0.5408	
	θ	106.7	107.3	
$[Co(\eta^3\text{-allyl})(CO)_2(N_2)]$	K			1 626.3
	k_i			41.7
	R			0.6796
	θ			101.0
$[Fe(\eta^4\text{-}C_4H_4)(CO)_3]$ [b]	K	1 635.0	1 621.6	1 627.6
	k_i	39.7	40.5	40.9
	R	0.3696	0.3301	0.3476
	θ	95.5 [c]	97.3 [c]	96.5 [c]
$[Fe(\eta^4\text{-}C_4H_4)(CO)_2]$ [b]	K	1 570.4	1 556.2	
	k_i	54.7	54.0	
	R	0.6546	0.6722	
	θ	102.1	101.3	
$[Fe(\eta^4\text{-}C_4H_4)(CO)_2(N_2)]$ [b]	K			1 596.6
	k_i			42.3
	R			0.7872
	θ			96.8

[a] See text for definition. [b] Data from ref. 23. [c] $\theta = 96.0°$ from electron diffraction studies and $\theta = 97.0°$ from crystallographic studies.

for $[Co(\eta^3\text{-allyl})(CO)_2]$ in Ar and CH_4 (Table 1) were used to calculate [25] energy-factored CO stretching (K) and interaction (k_i) force constants (Table 2). Relative intensities ($R = I_{A_1}/I_{B_1}$), obtained as for $[Co(\eta^3\text{-allyl})(CO)_3]$, were used to calculate bond angles for the $[Co(CO)_2]$ fragment from the expression $I_{sym}/I_{antisym} (= R) = \cot^2(\theta/2)$.[25]

Photolysis of $[Co(\eta^3\text{-allyl})(CO)_3]$ *in* N_2 *Matrices at* 12 K.—Infrared spectra from an experiment with $[Co(\eta^3\text{-allyl})(CO)_3]$ isolated at high dilution in a N_2 matrix are shown in Figure 2.

A period of u.v. irradiation with the medium-pressure mercury arc and filter A produced a spectrum [Figure 2(b)] containing three new bands at 2241.0, 2031.9, and 1980.5 cm^{-1}. The highest wavenumber band falls between the positions of ν(NN) in $[Ni(CO)_3(N_2)]$ (2 256 cm^{-1}, N_2 matrix) [27] and $[Mn(\eta^5\text{-}C_5H_5)(CO)_2(N_2)]$ (2 169 cm^{-1}, solution; 2 175 cm^{-1}, N_2 matrix) [23,28] and therefore can be assigned to a new complex containing a terminal dinitrogen species. The assignment of the remaining two bands as terminal CO stretching modes leads to the identification of the primary photoproduct as $[Co(\eta^3\text{-allyl})(CO)_2(N_2)]$. The band positions for $[Co(\eta^3\text{-allyl})(CO)_2(N_2)]$ (Table 1) were used to calculate [25] energy-factored CO stretching (K) and interaction (k_i) force constants (Table 2). The relative intensity of the two CO bands ($R = A'/A''$), obtained as described previously, gave a OC–Co–CO bond angle (θ) of 101 ± 1° (Table 2) from the expression $I_{sym}/I_{antisym} (= R) = \cot^2(\theta/2)$.[25] This angle is strikingly similar to the OC–Co–CO bond angle obtained for $[Co(\eta^3\text{-allyl})(CO)_3]$ (100°; Table 2).

Annealing the N_2 matrices, *i.e.* raising the temperature to *ca.* 30 K for a few minutes before re-cooling to 12 K in order

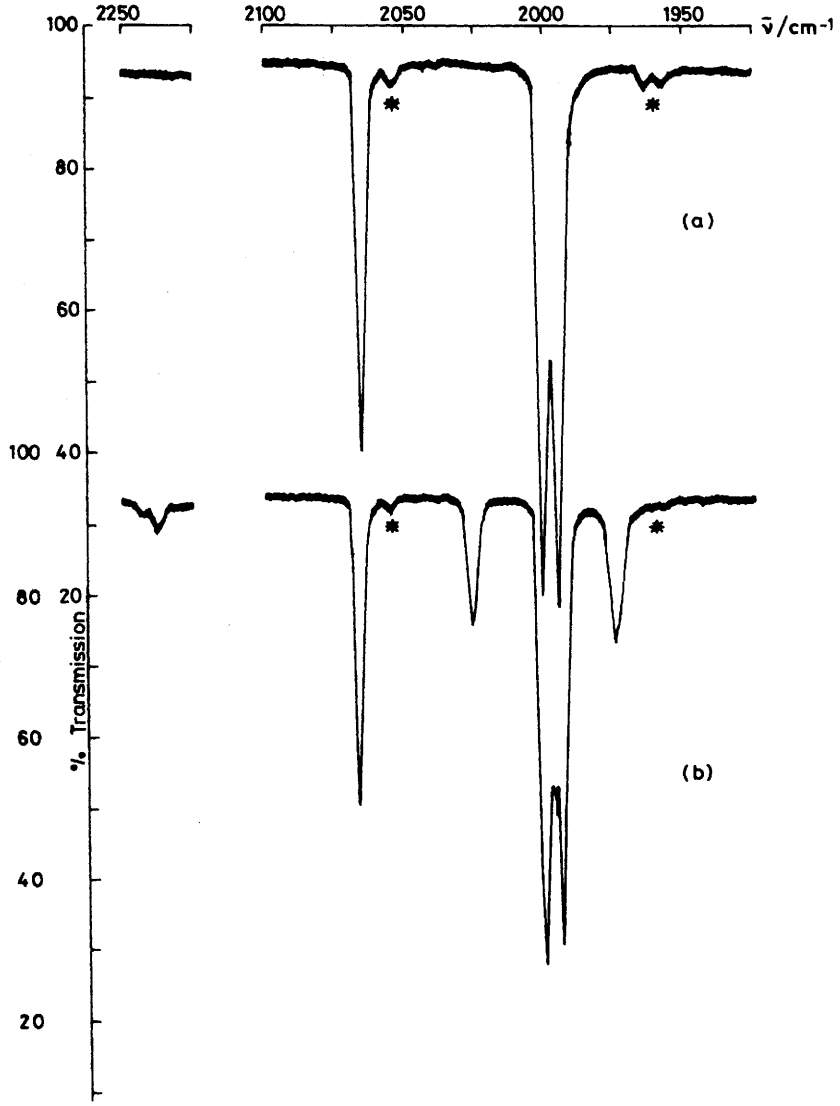

Figure 2. Infrared spectra from an experiment with [Co(η³-allyl)(CO)₃] isolated at high dilution in a N_2 matrix at 12 K: (a) after deposition, (b) after 90 min u.v. irradiation (filter A); bands marked with an asterisk (*) are due to [Co(η³-allyl)($^{12}CO)_2$(^{13}CO)] present in natural abundance

to run spectra, or long-wavelength irradiation (filter B), failed to reverse the forward reaction, in contrast to the behaviour in Ar and CH_4 matrices.

Photolysis of [Co(η³-allyl)(CO)₃] *in* CO *Matrices at* 12 K.—Infrared spectra from experiments with [Co(η³-allyl)(CO)₃] isolated at high dilution in CO matrices are shown in Figures 3 and 4.

The u.v. spectrum obtained for [Co(η³-allyl)(CO)₃] isolated in a CO matrix (Figure 5) indicated the possibility of a weak absorption band at *ca.* 400 nm. Long-wavelength irradiation (filter B) was carried out prior to irradiating into the more intense u.v. absorption bands. A period of visible range irradiation led to the destruction of the parent complex and the appearance of new absorption bands at 2103.0, 2037.6, 2020.9, and 2012.3 cm^{-1} [marked A in Figure 3(b)]. In a series of experiments using varying irradiation times the full set of bands was always present and they behaved similarly, having constant relative intensities. This behaviour is typical of bands which arise from a single product species and which must, on account of the dilution, be a mononuclear species. The shift of the new set of bands (Table 1) to higher wavenumbers than those for [Co(η³-allyl)(CO)₃] is analogous to the shift of product bands to higher wavenumbers when [Co(η⁵-C_5H_5)-(CO)₂] was irradiated in a CO matrix.[17] In this case the product was assigned as [Co(η³-C_5H_5)(CO)₃], *i.e.* a shift to higher wavenumbers for terminal CO stretching bands may be associated with an increase in the number of bound CO ligands. Consequently, the new photoproduct bands [marked A in Figure 3(b)] can probably be assigned as the terminal CO stretching bands of [Co(σ-allyl)$(CO)_4$] (see Discussion section),* where a change in hapticity for the allyl ligand

* Attempts to demonstrate conclusively by ^{13}CO labelling that the species contained a [Co$(CO)_4$] fragment were thwarted by: (*a*) the modest photoconversion together with the number of bands [Figure 3(b)], (*b*) the presence of $^{13}C^{16}O$ and $^{12}C^{18}O$ bands which blot out the 2 100—2 080 cm^{-1} region in mixed $^{12}CO/^{13}CO$ matrices containing sufficient ^{13}CO (^{12}CO : ^{13}CO = 1 : 1) to allow the possibility of generating enough of the enriched product species, and

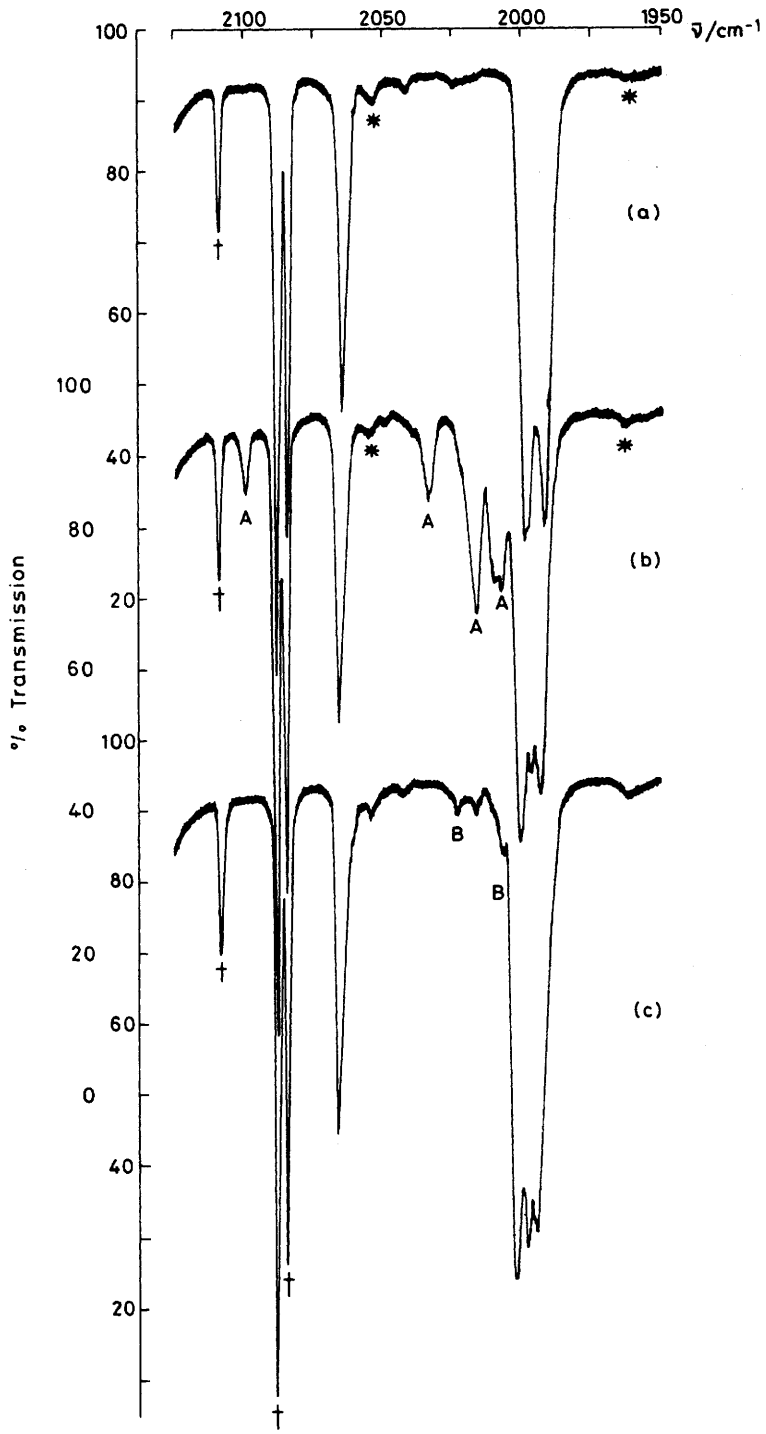

Figure 3. Infrared spectra from an experiment with [Co(η³-allyl)(CO)₃] isolated at high dilution in a CO matrix at 12 K: (a) after deposition, (b) after 20 min long wavelength irradiation (filter B), and (c) after 30 min u.v. irradiation (filter A); bands marked with a dagger (†) are due to $^{13}C^{16}O$ and $^{12}C^{18}O$ and those marked with an asterisk (*) are due to [Co(η³-allyl)($^{12}CO)_2(^{13}CO)$], all present in natural abundance

maintains the eighteen-electron configuration of the central cobalt atom.

Annealing failed to reverse the forward photoreaction but u.v. irradiation (filter A) led to the reduction of primary product bands (marked A), regeneration of bands due to [Co(η³-allyl)(CO)₃], and the appearance of two new weak bands [marked B in Figure 3(c): 2028.0 and 2009.9 cm^{-1}]. The latter pair of bands continued to grow slowly and with constant relative intensity during successive cycles of visible followed by u.v. irradiation, *i.e.* they were due to a further

(*c*) the overlap of bands in the lower wavenumber region with those of [Co(η³-allyl)($^{12}CO)_{3-n}(^{13}CO)_n$], produced by photochemical exchange in the matrix and also, surprisingly, arising from exchange of [Co(η³-allyl)($^{12}CO)_3$] with ^{13}CO in the gas phase prior to deposition of the matrix mixture on the cold window.

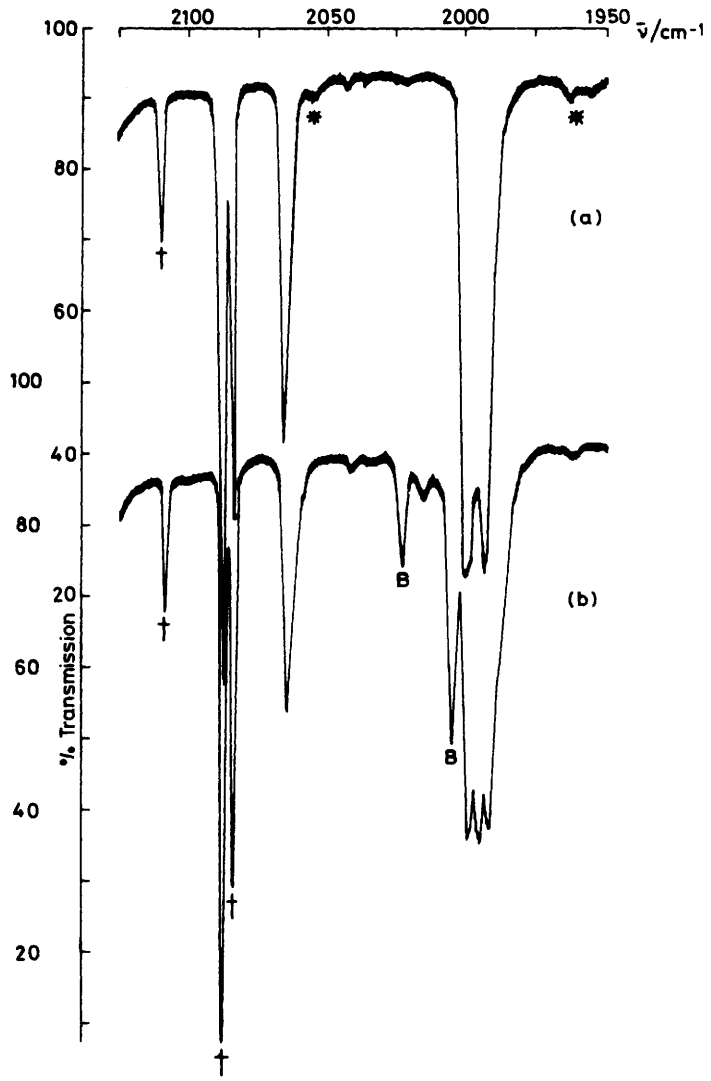

Figure 4. Infrared spectra from an experiment with [Co(η³-allyl)(CO)₃] isolated at high dilution in a CO matrix at 12 K: (a) after deposition and (b) after 30 min irradiation with the total output of the medium-pressure Hg arc, *i.e.* u.v. and long-wavelength irradiation; bands marked with a dagger (†) are due to $^{13}C^{16}O$ and $^{12}C^{18}O$ and those marked with an asterisk (*) are due to [Co(η³-allyl)($^{12}CO)_2$(^{13}CO)], all present in natural abundance

mononuclear photoproduct. At no time was this second photoproduct species formed directly from [Co(η³-allyl)(CO)₃] by irradiation with u.v. light (filter A) and, once formed, no reversal was observed either by annealing to 30 K or by irradiating at a variety of other wavelengths using other wavelength-selective materials.

As the pair of irreversible product bands (marked B) were apparently produced only after the formation of the primary photoproduct (bands marked A) and as a result of successive visible and u.v. irradiations, further experiments were carried out with simultaneous visible and u.v. irradiation using the Hg arc without filters. The spectrum obtained after such irradiation [Figure 4(b)] showed the direct production of the secondary product (bands marked B) in much higher yield than previously, whilst the primary product was absent. The positions and relative intensity of the two secondary photoproduct bands are very similar to those of [Co(CO)₄] formed on photolysis of [Co(CO)₃(NO)] in CO matrices at 20 K,[29] and by co-condensation of Co atoms with CO/Ar gas mixtures at 10—20 K.[30,31] Confirmation of the identity of the secondary photoproduct species as [Co(CO)₄] was afforded by an experiment when [Co(η³-allyl)(CO)₃] was irradiated with the unfiltered arc in a mixed $^{12}CO/^{13}CO$ matrix. The band positions [32] showed a good fit with those obtained previously for [Co($^{12}CO)_{4-n}$($^{13}CO)_n$] generated from [Co($^{12}CO)_3$(NO)] in mixed $^{12}CO/^{13}CO$ matrices.[29]

Discussion

The Identity and Structure of the Primary Photoproduct in CO Matrices.—Two experimental observations are crucial to the identification of the primary photoproduct in CO matrices: (*a*) that the formation of this species can be reversed to give back [Co(η³-allyl)(CO)₃], and (*b*) that the final removal of the allyl ligand produces a species with only *four* CO ligands. The former observation indicates that the allyl ligand is retained, *i.e.* [Co(allyl)($CO)_n$], while the latter observation indicates that $n \leqslant 4$. The shift of the bands of [Co(η³-allyl)(CO)₂] (Table 1) to lower wavenumbers than those of [Co(η³-allyl)(CO)₃] rules out this species, *i.e.* $n \neq 2$. The shift of the bands of [Co(allyl)($CO)_n$] to higher wavenumbers than those of [Co(η³-allyl)(CO)₃] is typical of the formation of a new species with

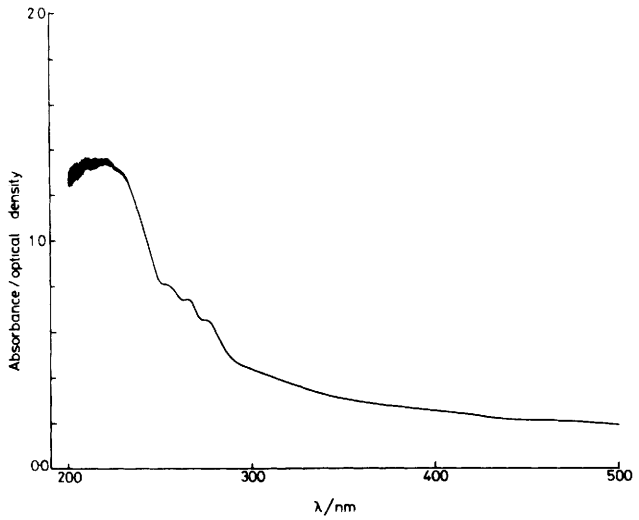

Figure 5. Ultraviolet–visible spectrum from an experiment with [Co(η³-allyl)(CO)₃] isolated at high dilution in a CO matrix at 12 K

additional CO ligands, *i.e.* $n = 4$. It remains, therefore, to determine the mode of co-ordination of the allyl ligand in [Co(allyl)(CO)₄].

Unlike Mn, for which both [Mn(σ-allyl)(CO)₅] and [Mn(η³-allyl)(CO)₄] are known stable complexes,[33] only [Co(η³-allyl)(CO)₃] and [Co(η³-perfluoroallyl)(CO)₃][34] have been isolated for Co. The latter complex, however, reacted with triphenylphosphine to give [Co(σ-perfluoroallyl)(CO)₃{P(C₆H₅)₃}] as a minor product.[34] In matrix isolation studies when species are formed which could have sixteen- or twenty-electron configurations and which contain ligands that can rearrange or change their hapticity, then rearrangement in order to achieve an eighteen-electron configuration occurs. For example, photolysis of [Mn(CH₃CO)(CO)₅] even in CO matrices at 12 K leads to the transient formation of [Mn(CH₃CO)(CO)₄] (sixteen-electron), but this species immediately goes on to [Mn(CH₃)(CO)₅] (eighteen-electron) by a methyl migration.[35] On this basis it seems probable that the primary photoproduct can be formulated as [Co(σ-allyl)(CO)₄] (eighteen-electron). This formulation is supported by the close correspondence of terminal CO stretching bands of this species [2103.0, 2037.6, 2020.9, and 2012.3 cm⁻¹; Figure 4(b)] with those of [Co(CH₃)(CO)₄] (2104.6w, 2035.5s, and 2018.5 cm⁻¹; n-hexane).[36]

Complexes of the type [Co(R)(CO)₄] and [Co(R_F)(CO)₄] (R_F = perfluoroallyl) adopt a trigonal bipyramidal structure with R or R_F in an axial position. Such a structure has C_{3v} symmetry in the case of [Co(CH₃)(CO)₄] with the three bands being assigned[36] the labels A_1 (2104.6), A_1 (2035.5), and E (2018.5 cm⁻¹). Complexes of the type [Co(R)(CO)₄] and [Co(R_F)(CO)₄], which have less symmetric R (or R_F) groups, also have their terminal CO stretching bands assigned as though the complexes had C_{3v} overall symmetry or have C_{3v} local symmetry for the [Co(CO)₄] fragment whereas C_s symmetry is strictly correct. For example, in the case of [Co(CF₃CF=CF)(CO)₄] the additional bands were assigned as arising from lifting of the degeneracy of the degenerate E mode, 2130.0m to A_1, 2068.1 to A_1, and 2059.8s + 2052.2s cm⁻¹ to E.[34] With regard to the four bands of [Co(σ-allyl)(CO)₄], the two upper bands (2103.0 and 2037.6 cm⁻¹) correspond remarkably well in position and intensity with the upper two bands of [Co(CH₃)(CO)₄] (2104.6 and 2035.5 cm⁻¹). The separation (*ca.* 8 cm⁻¹) between the lower two bands for [Co(σ-allyl)(CO)₄] (2020.9 and 2012.3 cm⁻¹) is similar to that observed for

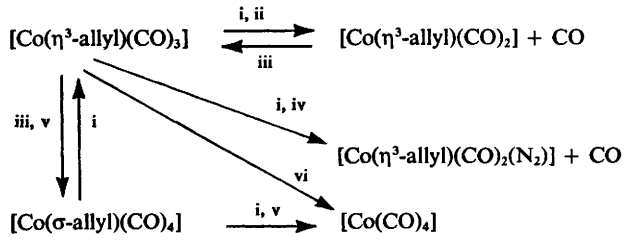

Scheme. i, *hν* (u.v.); ii, Ar, CH₄; iii, *hν* (visible); iv, N₂; v, CO; vi, *hν* (u.v.–visible)

a wide variety of asymmetric [Co(R)(CO)₄] and [Co(R_F)(CO)₄] complexes, *e.g.* [Co(CF₃CF=CF)(CO)₄] (7.6 cm⁻¹), and it also falls within the range of splitting arising from matrix effects,[24] *e.g.* the splitting of the lower band of [Co(η³-allyl)(CO)₃] in various matrices [Figures 1(a)—4(a)]. Taking the splitting as arising from matrix effects and/or some asymmetry, the weighted mean band position (2017.7 cm⁻¹) is now in close agreement with the position of the E mode of [Co(CH₃)(CO)₄] (2018.5 cm⁻¹). It is, therefore, proposed that [Co(σ-allyl)(CO)₄] adopts a trigonal bipyramidal structure with the σ-allyl ligand in the axial position, analogous to other [Co(R)(CO)₄] and [Co(R_F)(CO)₄] complexes, and with the [Co(CO)₄] fragment having C_{3v} local symmetry.

Reactions of [Co(η³-allyl)(CO)₃].—The photoreactions of [Co(η³-allyl)(CO)₃] in inert (Ar or CH₄) and reactive (N₂ or CO) matrices are summarised in the Scheme.

The ejection of CO in Ar and CH₄ matrices gives the species [Co(η³-allyl)(CO)₂] in good accord with the dissociation mechanism (S_N1) proposed from kinetic studies for the CO substitution reactions of [Co(η³-allyl)(CO)₃] in solution [4] and with theoretical predictions of dominant S_N1 character and high reactivity for [Co(η³-allyl)(CO)₃] as compared with low reactivity and the possibility of mixed S_N1/S_N2 pathways for [Fe(η⁴-C₄H₄)(CO)₃], [Mn(η⁵-C₅H₅)(CO)₃], and [Cr(η⁶-C₆H₆)(CO)₃].[7–10] The observation of [Co(σ-allyl)(CO)₄] in CO matrices together with the reversibility of the reaction [Co(η³-allyl)(CO)₃] + CO ⇌ [Co(σ-allyl)(CO)₄] and ^{1}H n.m.r. studies [12] on η³-allylmetal complexes suggests that there may be a contribution to the reactivity from the hitherto neglected S_N2 path. A reversible change in the hapticity of the allyl ligand in [Co(η³-allyl)(CO)₃] would create a site for the attack of a ligand (L) to form [Co(σ-allyl)(CO)₃(L)] followed by ejection of CO (or L) to give [Co(η³-allyl)(CO)₂(L)] {or [Co(η³-allyl)(CO)₃]}. Support for this path is afforded by the detection of [Co(σ-perfluoroallyl)(CO)₃{P(C₆H₅)₃}] in the reaction of [Co(η³-perfluoroallyl)(CO)₃] with triphenylphosphine.[34] Additional support for the possibility of a second path comes from the ready exchange of ^{13}CO with [Co(η³-allyl)(CO)₃] in a darkened matrix gas bulb prior to deposition on the cold window. Under similar circumstances, [Fe(η⁴-C₄H₄)(CO)₃], which is of almost comparable reactivity in other respects, showed no exchange.

The energy-factored CO stretching force constants and bond angles for [Co(η³-allyl)(CO)₃], [Co(η³-allyl)(CO)₂], and [Co(η³-allyl)(CO)₂(N₂)] (Table 2) may be compared with analogous data for [Cr(η⁶-C₆H₆)(CO)₃], [Mn(η⁵-C₅H₅)(CO)₃], and [Fe(η⁴-C₄H₄)(CO)₃] and species derived from them, which have been the subjects of theoretical calculations.[7,9,10,37] Representative data for [Fe(η⁴-C₄H₄)(CO)₃], [Fe(η⁴-C₄H₄)(CO)₂], and [Fe(η⁴-C₄H₄)(CO)₂(N₂)] are given in Table 2.

The principal stretching force constant (K; Ar matrices) data for [Co(η³-allyl)(CO)₃] and [Co(η³-allyl)(CO)₂] fit well into the calculated trends of decreasing M–C(O) bond order (Cr > Mn > Fe > Co) and increasing C–O bond order

(Cr < Mn < Fe < Co) across the series. It was this trend which led to the predicted [7,9,10] dominance of the S_N1 path in substitution reactions of [Co(η^3-allyl)(CO)$_3$].

For Cr, Mn, and Fe complexes the values of the interaction (k_i) force constants and bond angles (θ) were approximately constant for the [M(CO)$_3$] and [M(CO)$_2$] series of fragments respectively.[23,37] Data for [Co(η^3-allyl)(CO)$_3$] and [Co(η^3-allyl)(CO)$_2$] species (Table 2) are consistent with those for other [M(CO)$_3$] and [M(CO)$_2$] fragments. Additionally the values of k_i and θ for [M(CO)$_2$(N$_2$)] fragments showed a good correspondence with such parameters for the parent [M(CO)$_3$] fragments,[23,37] as is to be expected when a N_2 ligand replaces a CO ligand and the pseudo-[M(CO)$_3$] fragment geometry is retained.

Values of ν_{NN} for [M(CO)$_2$(N$_2$)] species increased in the series Cr (2148.4 cm^{-1}) < Mn (2176.3 cm^{-1}) < Fe (2206.8 cm^{-1}) and this was correlated with increasing NN bond order and decreasing M–N(N) bond order.[23,37] The value of ν_{NN} for [Co(η^3-allyl)(CO)$_2$(N$_2$)] (2241.0 cm^{-1}) is again consistent with the predicted trend. In view of the failure [38] to prepare [Fe(η^4-C$_4$H$_4$)(CO)$_2$(N$_2$)] (ν_{NN} = 2206.8 cm^{-1}), even when it was known to exist in a matrix, it seems unlikely that [Co(η^3-allyl)(CO)$_2$(N$_2$)] (ν_{NN} = 2241.0 cm^{-1}) will ever be synthesised because its M–N(N) bond order is even lower than that of [Fe(η^4-C$_4$H$_4$)(CO)$_2$(N$_2$)].

In future work we will investigate the photoreactions of other allylmetal complexes where both σ-allyl and η^3-allyl bonding is found for the same metal, *e.g.* [Mn(σ-allyl)(CO)$_5$] and [Mn(η^3-allyl)(CO)$_4$].

Conclusions

Matrix isolation studies have shown that photolysis of [Co(η^3-allyl)(CO)$_3$] in Ar and CH$_4$ matrices at 12 K leads to a co-ordinatively unsaturated species, [Co(η^3-allyl)(CO)$_2$], in accordance with the dissociative (S_N1) path proposed for CO exchange and substitution reactions. Photolysis in CO matrices leads to a species with an additional CO ligand, [Co(σ-allyl)(CO)$_4$]. The detection of this species and the reversibility of the reaction (i) suggest a contribution to the reactivity of [Co(η^3-allyl)(CO)$_3$] from the hitherto neglected

$$[Co(\eta^3\text{-allyl})(CO)_3] + CO \rightleftharpoons [Co(\sigma\text{-allyl})(CO)_4] \quad (i)$$

associative (S_N2) path, and that further kinetic studies of [Co(η^3-allyl)(CO)$_3$] should be undertaken to test this hypothesis.

Acknowledgements

We thank the S.R.C. for support (to A. J. R.) and for a studentship (to D. J. T.).

References

1 R. J. Angelici, *Organomet. Chem. Rev.*, 1968, **3**, 173.
2 D. A. Brown, 'Inorganic Chemistry, Series 2,' MTP International Reviews of Science Series, Butterworth, London, 1975, vol. 9.
3 J. P. Day, F. Basolo, and R. G. Pearson, *J. Am. Chem. Soc.*, 1968, **90**, 6927.
4 R. F. Heck, *J. Am. Chem. Soc.*, 1963, **85**, 655; 1965, **87**, 2572.
5 E. M. Thorsteinson and F. Basolo, *J. Am. Chem. Soc.*, 1966, **88**, 3929.
6 G. Cardaci and S. M. Margia, *J. Organomet. Chem.* 1970, **25**, 483.
7 D. A. Brown, H. L. Clarke, and N. J. Fitzpatrick, *J. Organomet. Chem.*, 1973, **47**, C11.
8 H. L. Clarke, *J. Organomet. Chem.*, 1974, **80**, 369.
9 D. A. Brown, N. J. Fitzpatrick, and N. J. Mathews, *J. Organomet. Chem.*, 1975, **88**, C27.
10 N. J. Fitzpatrick, J-M. Savariault, and J-F. R. Labarre, *J. Organomet. Chem.*, 1977, **127**, 325.
11 H. G. Schuster-Woldan and F. Basolo, *J. Am. Chem. Soc.*, 1966, **88**, 1659.
12 J. W. Fuller, M. E. Thomsen, and M. J. Mattina, *J. Am. Chem. Soc.*, 1971, **93**, 2642 and refs. therein.
13 R. Baker, *Chem. Rev.*, 1973, **73**, 487.
14 H. Bönnemann, *Angew. Chem., Int. Ed. Engl.*, 1973, **12**, 964.
15 C. Masters, 'Homogeneous Transition-metal Catalysis,' Chapman and Hall, London, 1981.
16 J. K. Burdett, *Coord. Chem. Rev.*, 1978, **27**, 1.
17 O. Crichton, A. J. Rest, and D. J. Taylor, *J. Chem. Soc., Dalton Trans.*, 1980, 167.
18 G. Ellerhorst, W. Gerhartz, and F-W. Grevels, *Inorg. Chem.*, 1980, **19**, 67.
19 R. F. Heck and D. S. Breslow, *J. Am. Chem. Soc.*, 1961, **83**, 1097.
20 R. Seip, *Acta Chem. Scand.*, 1972, **26**, 1966.
21 E. W. Abel, M. A. Bennett, R. Burton, and G. Wilkinson, *J. Chem. Soc.*, 1958, 4559.
22 R. H. Hooker and A. J. Rest, *J. Chem. Soc., Dalton Trans.*, 1982, 2029.
23 A. J. Rest, J. R. Sodeau, and D. J. Taylor, *J. Chem. Soc., Dalton Trans.*, 1978, 651.
24 A. J. Barnes, in 'Matrix Isolation Spectroscopy,' N.A.T.O. Advanced Study Institute Series, eds. A. J. Barnes, W. J. Orville-Thomas, A. Müller, and R. Gaufrés, Reidel, London, 1981, ch. 2.
25 P. S. Braterman, 'Metal Carbonyl Spectra,' Academic Press, London, 1975.
26 T. Chiang, R. C. Kerber, S. D. Kimball, and J. W. Lauher, *Inorg. Chem.*, 1979, **18**, 1687.
27 A. J. Rest, *J. Organomet. Chem.*, 1972, **40**, C76.
28 D. Sellmann, *Angew. Chem., Int. Ed. Engl.*, 1971, **10**, 919.
29 O. Crichton, M. Poliakoff, A. J. Rest, and J. J. Turner, *J. Chem. Soc. Dalton, Trans.*, 1973, 1321.
30 G. A. Ozin, in 'Vibrational Spectra of Trapped Species,' ed. H. Hallam, Wiley, London, 1973.
31 L. A. Hanlan, H. Huber, E. Kündig, B. R. McGarvey, and G. A. Ozin, *J. Am. Chem. Soc.*, 1975, **97**, 7054.
32 D. J. Taylor, Ph.D. Thesis, University of Southampton, 1980.
33 H. D. Kaesz, R. B. King, and F. G. A. Stone, *Z. Naturforsch., Teil B*, 1960, **15**, 682.
34 K. Stanley and D. W. McBride, *Can. J. Chem.*, 1975, **53**, 2537.
35 T. M. McHugh and A. J. Rest, *J. Chem. Soc., Dalton Trans.*, 1980, 2323.
36 G. Bor, *Inorg. Chim. Acta*, 1967, **1**, 82.
37 N. J. Fitzpatrick, A. J. Rest, and D. J. Taylor, *J. Chem. Soc., Dalton Trans.*, 1979, 351.
38 I. Fischler, K. Hildenbrand, and E. A. Koerner von Gustorf, *Angew. Chem., Int. Ed. Engl.*, 1975, **14**, 54.

Received 6th September 1982; *Paper* 2/1538